IN VIVO EXPRESSION OF PERFORIN BY CD8+ LYMPHOCYTES DURING AN ACUTE VIRAL INFECTION

By LUCY H. Y. YOUNG, LINDA S. KLAVINSKIS,*
MICHAEL B. A. OLDSTONE,* AND JOHN DING-E YOUNG‡

*From the Massachusetts Eye and Ear Infirmary, Harvard Medical School, Boston,
Massachusetts 02114; the *Department of Immunology, Scripps Clinic and Research Foundation,
La Jolla, California 92037; and the ‡Laboratory of Cellular Physiology and Immunology,
The Rockefeller University, New York, New York 10021*

A pore-forming protein (PFP;[1] also termed perforin or cytolysin) has previously been identified in the granules of CTL and NK cells (1–4). In the presence of calcium, isolated PFP/perforin lyses a variety of target cells nonspecifically. The pore formation model for cell killing, taking into account the lytic function of perforin, is attractive in that it provides a unifying concept that explains cytotoxicity mediated by both CTL and NK cells. Since all previous biochemical analyses of perforin have been conducted with CTL and NK cells propagated in long-term cultures in vitro, it is not clear whether perforin is expressed in vivo by lymphocytes actively engaged in cell-mediated killing. Moreover, the reported absence of measurable amounts of perforin in CTL primed in vivo (5–7) has led to the suggestion that expression of perforin is inextricably driven by IL-2 in vitro, raising the question as to whether this mechanism of lymphocyte-mediated killing occurs in vivo.

To address this issue, we investigated the expression of perforin in animals undergoing acute viral infections. CTL and NK cells have long been associated with antiviral immunity (8–12), and in some instances have been implicated directly in the development of immunopathologic injury (11–14). We chose to analyse the murine infection produced by lymphocytic choriomeningitis virus (LCMV), a member of the arenavirus family. During acute infection it produces intense but localized inflammatory changes, like leptomeningitis and choroiditis or hepatitis, with massive accumulation of CTL and NK cells in the diseased tissues (11–14). Using two strains of LCMV (one primarily causing leptomeningitis and the other primarily hepatitis) and by means of immunohistochemical analysis, we show here that perforin is found

abundantly in vivo, in lymphocytes of both the CTL and NK cell phenotypes. Thus, perforin may play an important role in limiting viral infections by lysing virus-infected cells and in underlying the immunopathology of viral disorders.

Materials and Methods

Mice.   6–8-wk-old BALB/C/byj (H-2^d), C57BL/6 (H-2^b), and SWR/J (H-2^q) mice were obtained from the breeding colony at the Research Institute of Scripps Clinic (La Jolla, CA).

Antibodies.   Three rabbit polyclonal anti–mouse perforin antisera, prepared as described (15, 16), were used. These three antisera were prepared against different batches of purified perforin but gave similar staining patterns at dilutions ranging from 1:50 to 1:200. These antisera were raised against the nonreduced form of perforin and have been shown not to react with either human (15) or murine (unpublished) complement components. In some experiments IgG preparations were obtained from these antisera by affinity chromatography on protein A–agarose (Boehringer Mannheim Biochemicals, Indianapolis, IN) (15). Polyclonal antigangliotetraosylceramide (anti–asialo GM$_1$) antisera were purchased from Wako Chemicals (Dallas, TX) and were used at a dilution of 1:800. Hybridoma supernatants containing mAbs specific for CD4 (TIB 207, rat IgG2b), CD8 (TIB 105, rat IgG2a), Thy-1 (B5-3, rat IgG2b), a common leukocyte antigen (TIB 122, rat IgG 2a), and a macrophage antigen (F4/80, rat IgG2b) were generously obtained from Dr. R. Steinman's laboratory (The Rockefeller University, New York) and were used at 1:5 dilutions. TIB 105 (anti-CD8) IgG 2a was obtained by affinity purification, as above. The origins and characteristics of these antibodies have been summarized elsewhere (17). A mouse mAb specific for NK 1.1 alloantigen (H-2^b) (18) was generously provided by Dr. R. D. Welsh, University of Massachusetts Medical School, Worcester, MA.

Viruses.   Two strains of LCMV were used: the neurotropic isolate, Armstrong CA 1371, (LCMV-ARM, clone 53b) and the hepatotropic isolate, WE (LCMV-WE, clone 54). The viruses were cloned and plaque purified three times on Vero cells. Virus stocks were thereafter grown in BHK-21 cells as described (19).

Virus Infection In Vivo.   Groups of five mice each were infected intraperitoneally with 2 × 10^5 plaque-forming units (PFU) of LCMV-WE, or intracerebrally with 5 × 10^2 PFU of LCMV-ARM. On the days indicated, mice were anaesthetized and perfused with 4% paraformaldehyde in 0.1 M sodium phosphate buffer. Tissues were post-fixed 1 h at room temperature, cryoprotected in 18% sucrose overnight, snap-frozen in Tissue-Tek O.C.T. (Miles Scientific, Naperville, IL), and prepared for immunohistochemistry as described (20).

Immunohistochemistry and Histologic Procedures.   Cryostat sections of brain or liver (10–12-μm thick) were cut and dried onto gelatin-coated slides, preincubated with 15% normal goat serum (NGS) in PBS for 1 h at 4°C, and incubated with the indicated antibodies overnight at 4°C. After washing for 1 h, the slides were incubated with either biotin-conjugated goat anti–rabbit or anti–rat IgG (Boehringer Mannheim Biochemicals) overnight at 4°C for immunoperoxidase staining or with FITC-conjugated goat anti–rabbit or anti–rat IgG (Boehringer Mannheim Biochemicals) for 1 h at 4°C for immunofluorescence staining. For monoclonal anti–NK 1.1, slides were blocked first with unlabeled goat anti–mouse IgG before anti–NK 1.1 staining, which was then followed by staining with FITC-goat anti–mouse IgG (Boehringer Mannheim Biochemicals). The slides were washed for 1 h. Those prepared for immunoperoxidase staining were first incubated for 30 min in 0.3% H$_2$O$_2$ in PBS to quench endogenous peroxidase activity and washed in several changes of PBS. The sections were then incubated with avidin-biotinylated peroxidase complex (ABC-immunoperoxidase kit, Vector Laboratories, Inc., Burlingame, CA, prepared according to the manufacturer's instruction) for 1 h at 4°C, washed, and reacted with diaminobenzidine tetrahydrochloride (0.5 mg/ml; Polysciences, Inc., Warrington, PA). After peroxidase reaction, the slides were washed, dehydrated in increasing concentrations of ethanol, and mounted in Permount (Fisher Scientific Co., Pittsburgh, PA). The slides prepared for immunofluorescence staining were mounted in glycerol and viewed with fluorescence optics.

For double-labeling immunofluorescence staining, NGS-blocked slides were incubated with a mixture of monoclonal rat anti-CD8 and polyclonal rabbit anti-PFP (or anti–asialo GM$_1$)

antisera as before. After washing, the slides were incubated with FITC-conjugated goat anti-rat IgG and rhodamine isothiocyanate (RITC)-conjugated goat anti-rabbit IgG for 1 h at 4°C. In preliminary specificity control experiments, these labeled secondary antibodies were tested separately against sections stained with primary IgG of mismatched species: no specific staining was obtained (data not shown). For anti-asialo GM₁ and antiperforin staining, a serial double-labeling protocol was used, e.g., slides were first stained with anti-PFP antiserum, counterstained with RITC-conjugated goat anti-rat IgG as before, washed, and then blocked with unlabeled goat anti-rabbit Ig (Cappel Laboratories, Malvern, PA) at 40 µg/ml for 2 h. After additional washes, slides were stained with anti-asialo GM₁ antiserum, followed by washing and staining with FITC-conjugated goat anti-rabbit IgG. The blocking performed with unlabeled goat anti-rabbit Ig after the first round of staining was sufficient to remove all unreacted sites, since addition of FITC-conjugated goat anti-rabbit IgG before anti-asialo GM₁ antiserum did not produce any specific signal (not shown). Additional controls included the direct use of fluoresceinated IgGs specific for perforin (polyclonal IgG) and CD8 (monoclonal) for immunofluorescent staining. Staining patterns were similar to those obtained by indirect immunofluorescence.

For hematoxylin and eosin (H&E) staining, tissues were formalin fixed, embedded in paraffin, and stained as described (21).

Cerebrospinal Fluid (CSF) Sampling and Immunoblot Analysis. Aliquots of CSF were obtained from the cisterna magna of mice that had been exsanguinated under anaesthesia, as described (22). Cells in CSF were collected by centrifugation, washed three times in PBS, lysed in PBS containing 1% NP-40, and processed for immunoblot analysis using 10% SDS-polyacrylamide gels, exactly as described (15, 16). Blots were reacted with antiperforin antiserum at 1:50 dilution.

Results

Mononuclear Cell Infiltration Observed During LCMV Infection. Two strains of LCMV were used: Armstrong (LCMV-ARM) and WE (LCMV-WE). These have been shown to produce distinct pathologies, with choriomeningitis predominantly associated with LCMV-ARM and hepatitis with LCMV-WE. Groups of C57BL/6 and SWR/J mice at 8 wk of age were inoculated with LCMV-ARM or LCMV-WE (see Materials and Methods). At days 4, 5, and 6 (and 7 for C57BL/6) post-infection, brains or livers were processed for histological and immunohistochemical analysis. The brains of mice inoculated with LCMV-ARM revealed marked mononuclear cell infiltration of the meninges (compare Fig. 1, *a* vs. *b*) and choroid plexus (compare Fig. 1, *c* vs. *d*). The livers of mice inoculated with LCMV-WE also showed extensive mononuclear cell infiltration (Fig. 1, *e* vs. *f*). The inflammatory changes seen in SWR/J mice were more pronounced and occurred 1-2 d earlier than those observed in C57BL/6 mice. Mononuclear cell infiltrations peaked on days 5-6 for SWR/J mice and on day 7 for C57BL/6 mice. At the viral doses used here, infected SWR/J mice died on days 6-7, while C57BL/6 mice died on days 8-9.

Phenotypes of Lymphocyte Subsets in Infiltrates. Several mAbs were used to assess the phenotypes of leukocytes present in the brains of C57BL/6 and SWR/J mice infected with LCMV-ARM. Staining of virus-infected brains with mAbs directed against a common leukocyte antigen (not shown) or Thy-1 (Fig. 2 *a*), using the ABC-immunoperoxidase method, confirmed the presence of lymphocytes and other leukocytes infiltrating the meninges and choroid plexus. Other lymphocyte markers expressed on infiltrating lymphocytes found in the brain include CD8 (Fig. 2 *b*), asialo GM₁ (Fig. 2 *c*), and CD4 (Fig. 2 *d*). The relative distribution of these markers in virus-infected SWR/J and C57BL/6 mice is shown in Table I.

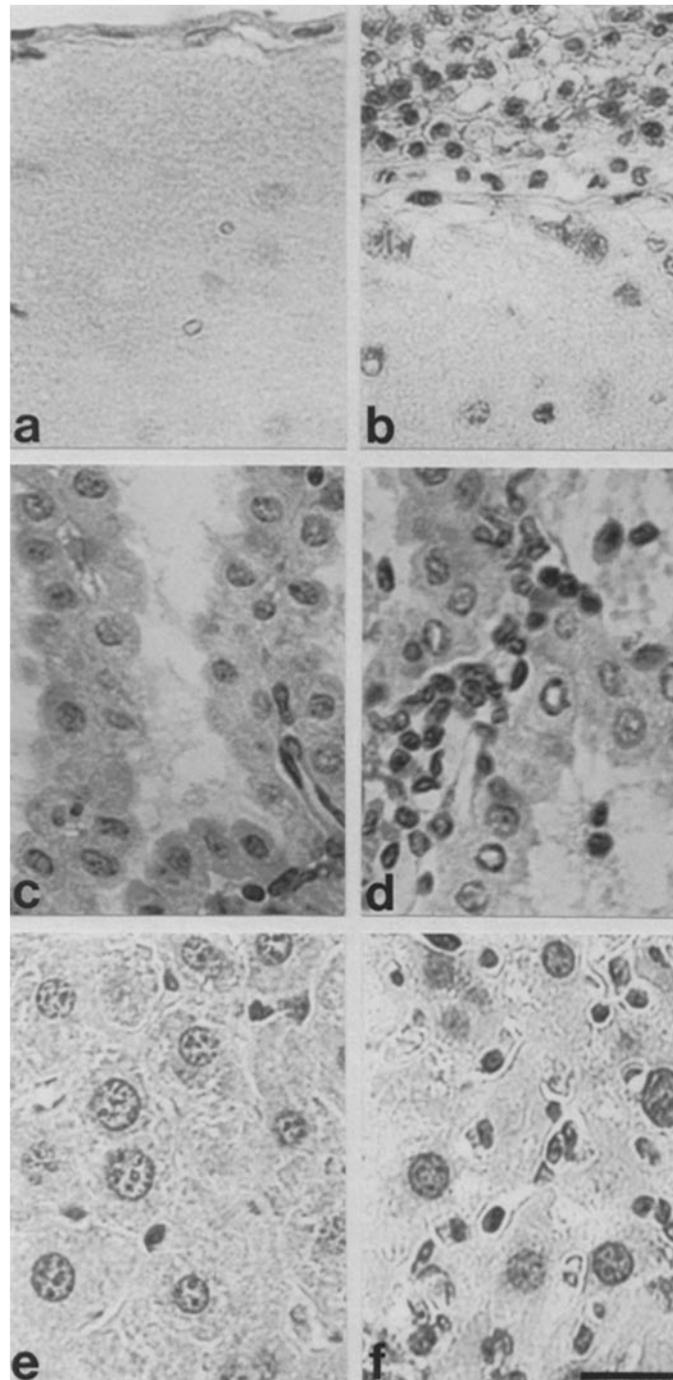The predominant markers found on infiltrating lymphocytes were CD8 (Lyt-2)

FIGURE 1. Histological analysis of normal and LCMV-infected mice using H&E staining. (a) Normal meninges and cortex; (b) brain of LCMV-ARM-infected mouse, showing marked thickening of meninges secondary to mononuclear cell infiltration; (c) normal choroid plexus; (d) in-
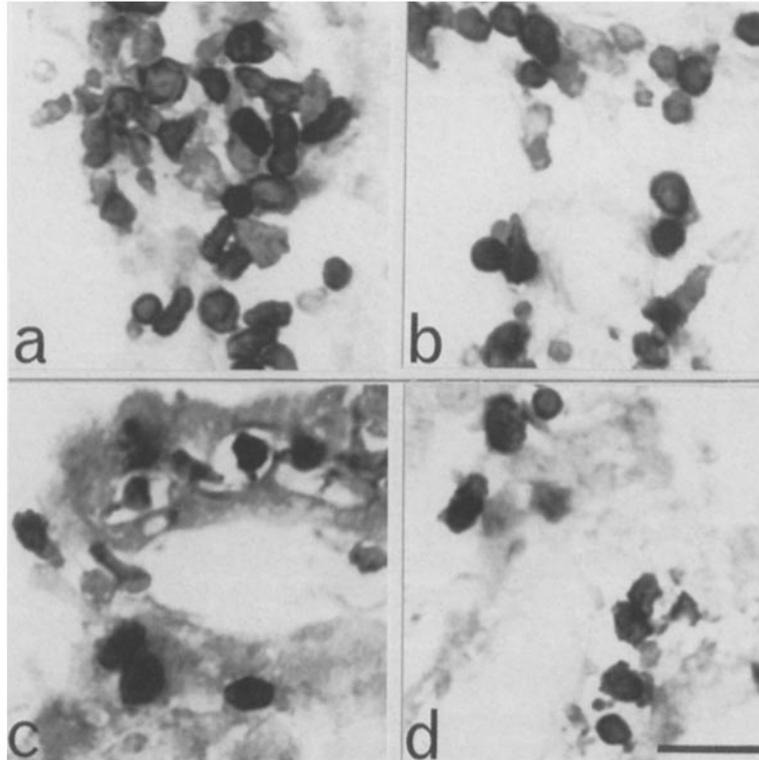
FIGURE 2.   Immunoperoxidase staining of LCMV-ARM-infected brain with leukocyte markers: (a) rat anti–mouse Thy-1; (b) rat anti–mouse CD8; (c) rabbit anti–asialo GM_1; and (d) rat anti–mouse CD4. Sections were obtained from a SWR/J mouse on day 5 post-infection. Bar = 21 μm.

and asialo GM_1 (Table I). Asialo GM_1 is a marker mainly found on NK cells but may also be present on activated T cells and macrophages (14, 23, 24). $CD8^+$ and asialo GM_1^+ cells increased sharply during the course of infection, with ~70–85% of lymphocytes becoming positive for these two markers during the terminal stages of infection (Table I). $CD8^+$ and asialo GM_1^+ cells typically contained reniform nuclei, high cytoplasm-to-nucleus ratios, and abundant cytoplasmic granules, a morphology consistent with that of large granular lymphocytes (LGL).

The simultaneous presence of large numbers of $CD8^+$ and asialo GM_1^+ LGL during LCMV infection suggested that the asialo GM_1^+ cells were also predominantly $CD8^+$. This inference was confirmed by double-labeling immunofluores-

fection as in (b), showing cellular infiltration of choroid plexus; (e) normal liver; (f) liver of LCMV-WE-infected mouse, revealing marked cellular infiltration. The brain sections (b and d) were obtained from infected C57BL/6 mice on day 7 post-infection and the liver section (f) from a SWR/J mouse on day 7 post-infection. Bar = 21 μm.

TABLE I

Relative Distribution of Phenotypic Markers among the Infiltrating
Lymphocytes Found in the Brains of Mice Infected with LCMV-ARM

Mice	Days post-infection	Percentage of cells that are:		
		CD4$^+$	CD8$^+$	asialo GM$_1$$^+$
SWR/J	4	45	50	52
	5	30	62	65
	6	15	81	85
C57BL/6	4	55	35	40
	5	43	51	53
	6	33	62	65
	7	23	68	76

The doses of LCMV-ARM used for infection are given in Materials and Methods.
A total of 200 cells were enumerated from each animal. Numbers represent averages of three animals.

cence analysis (Fig. 3). Approximately 85% of CD8$^+$ cells (ranging between 80 and 90% in different sections) also colabeled with asialo GM$_1$. The remaining double-label-negative cell population was distributed about equally between CD8$^+$/asialo GM$^-$ (Fig. 3, a and b, arrows) and CD8$^-$/asialo GM$^+$ (Fig. 3, c and d, arrowheads) cells. CD8$^+$ cells were CD4$^-$ and predominantly Thy-1$^+$ (staining done on adjacent sections, data not shown).

The small population of CD8$^-$/asialo GM$_1$$^+$ cells appeared to correspond to NK cells, as indicated by the presence of the NK-specific alloantigen NK 1.1 (18) in brain
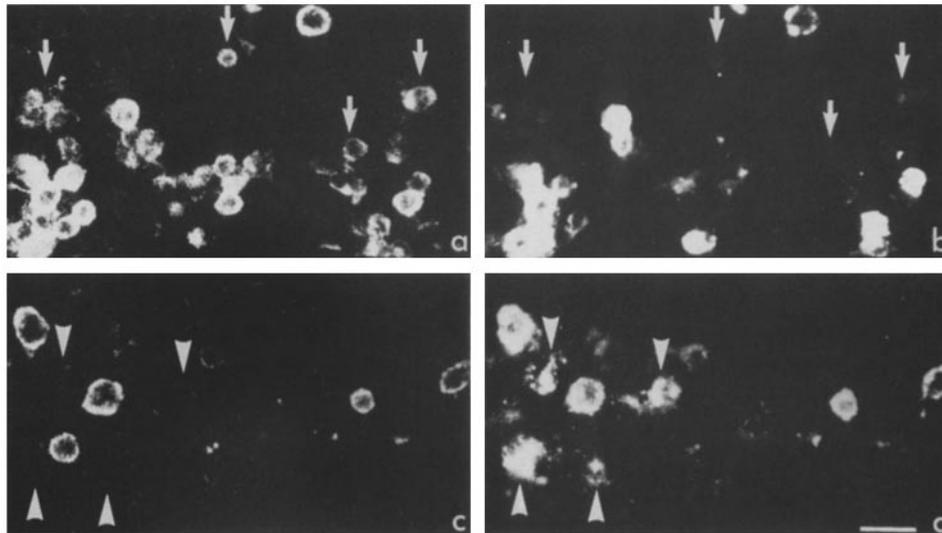

FIGURE 3.   Double-labeling immunofluorescence of cryostat sections of LCMV-ARM-infected brain with anti-CD8 (a, c; fluorescein) and anti–asialo GM$_1$ (b, d; rhodamine). The arrows in a and b indicate CD8$^+$/asialo GM$_1$$^-$ cells, while the arrowheads in c and d indicate CD8$^-$/asialo GM$^+$ cells. Sections were obtained from a SWR/J mouse on day 5 post-infection. Bar = 18 μm.
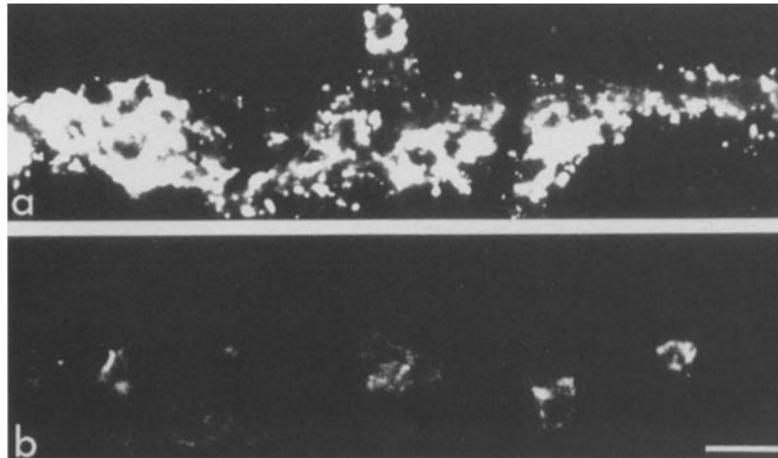
FIGURE 4.   Double-labeling immunofluorescence of a cryostat section of LCMV-ARM-infected brain with anti-asialo GM_1 antiserum (top; fluorescein) and F4/80 rat antimacrophage mAb (bottom; rhodamine). The section was obtained from a SWR/J mouse on day 5 post-infection. Bar = 18 μm.

sections of infected C57BL/6 mice that also colabeled for asialo GM_1 (data not shown). About 10–20% of asialo GM_1^+ cells also colabeled as NK 1.1^+ (not shown). To rule out the possibility that asialo GM_1^+ cells might represent macrophages, double-labeling studies were carried out using the macrophage-specific mAb F4/80 and anti–asialo GM_1 antiserum (Fig. 4). Asialo GM_1^+ cells were predominantly $F4/80^-$.

Expression of Perforin in Tissues of Virus-infected Mice.   Three different antiperforin polyclonal antisera with high specificity (15, 16) were used to stain sections of LCMV-infected animals. The perforin antigen was found to be absent from resident tissues of mice. However, a large number of perforin-positive cells were found at the sites of virus-induced inflammation (Fig. 5). In the brains of animals infected with LCMV-ARM, perforin-positive cells were seen usually located deep in the thickened meninges, in close proximity to the adjacent cortex. All perforin-positive cells displayed the LGL morphology, with intense staining of their cytoplasmic granules (Fig. 5). About 80–90% of all perforin-positive cells colabeled as $CD8^+$ (Fig. 6, *a* and *b*) or as asialo GM_1^+ (Fig. 6, *c* and *d*). However, only 25–30% of $CD8^+$ cells were also perforin-positive. After infection with LCMV-ARM, the number of perforin-positive cells peaked on day 5 for SWR/J mice and day 7 for C57BL/6.

Perforin-positive cells were also seen in liver sections of mice infected with LCMV-WE (Fig. 7). As in the brain, the majority of the lymphocytes was $CD8^+$/asialo $GM1^+$/$Thy-1^+$/$CD4^-$. A small proportion of the cells was also $CD8^-$/asialo $GM1^+$/$CD4^-$/NK 1.1^+ (in C57BL/6 mice) and $F4/80^-$, possibly representing NK cells. The majority of perforin-positive cells also colabeled as $CD8^+$ (Fig. 7). However, the proportion of perforin-positive cells as a fraction of total $CD8^+$ cell population was only of the order of 15% in LCMV-WE-infected livers under the conditions studied here.
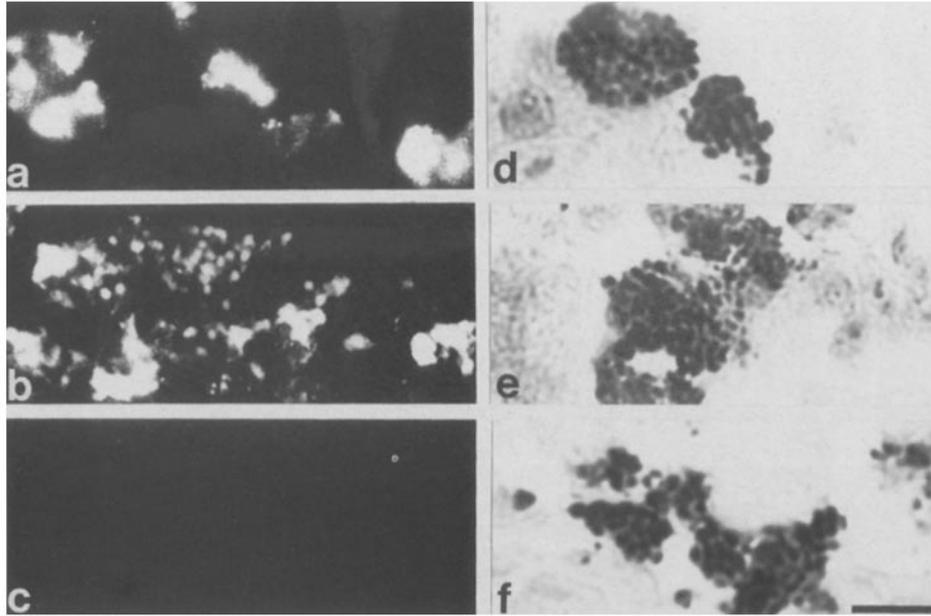
FIGURE 5.   Immunofluorescent staining (*left*) and ABC-immunoperoxidase staining (*right*) of frozen sections of LCMV-ARM-infected brains with rabbit anti-PFP/perforin antiserum (*a*, *b*, *d-f*) and pre-immune serum (*c*). Selected images are shown here of frozen sections obtained from SWR/J mice on day 5 post-infection. Note the intense granularity of stain seen in some cells (*b*, *d-f*). Bar = 12 μm (*a-c*) and 9 μm (*d-f*).
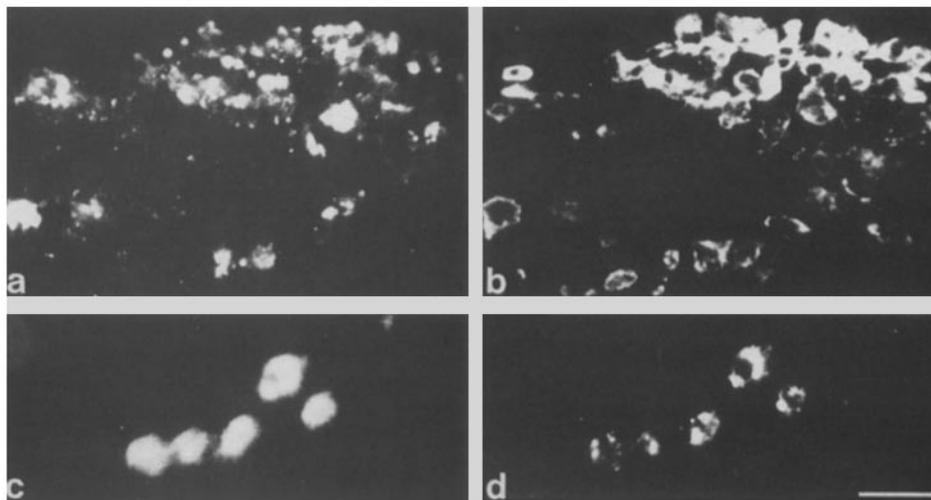

FIGURE 6.   Double-labeling immunofluorescence of frozen sections of an LCMV-ARM-infected brain with antiperforin antiserum (*a*; fluorescein) and anti-CD8 mAb (*b*; rhodamine) and antiperforin (*c*; fluorescein) and anti–asialo GM₁ (*d*; rhodamine) antisera. Bar = 28 μm.
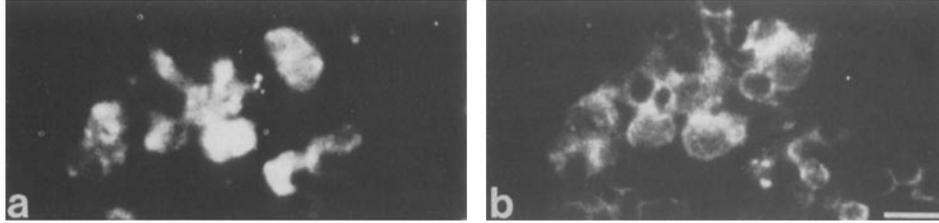
FIGURE 7. Double-labeling immunofluorescence of a frozen section of LCMV-WE-infected liver with antiperforin (a) and anti-CD8 (b) antisera. Note that perforin-positive cells colabel with the CD8 marker. Bar = 15 μm.

Specificity of Antiperforin Staining. To verify the specificity of staining obtained with the polyclonal antiperforin antisera used here, cells obtained from the CSF of C57BL/6 mice infected with LCMV-ARM (see Materials and Methods) were submitted to immunoblot analysis with these antisera. The results for one of the three antisera are shown in Fig. 8. A faint reactive band of 70 kD was observed in cells collected on day 3 post-infection (Fig. 8, lane *1*), while a much stronger band was observed in the same number of cells by day 7 (lane *2*), in accord with the time course of appearance of perforin-positive cells in brain sections. The position of this reactive band was identical to that of partially purified perforin reacted with the same antiserum (not shown). Preimmune serum did not react with any protein band of CSF-derived cells (Fig. 8, lanes *3* and *4*). Perforin-specific antisera also did not react with murine serum proteins (not shown), ruling out the possibility of any immunological crossreactivity with complement components. It should be pointed out that, to date, crossreactivities between perforin and complement components have been observed only when the immunogens/antigens used are disulfide reduced (15).

Discussion

The results presented here demonstrate for the first time the presence of PFP/perforin antigen in tissues of animals undergoing an acute viral infection. To date, all previous studies on perforin have been performed with effector lymphocytes that have been cultured and maintained in vitro. This fact has fueled speculation that perforin may represent a product of cultured lymphocytes only, and not of CTL that have been primed in vivo (5-7). Our results demonstrate that perforin is in
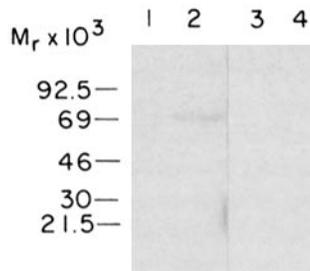

FIGURE 8. Immunoblot analysis with antiperforin antiserum. Cells were obtained from the CSF of LCMV-ARM-infected C57BL/6 mice, on days 3 (lanes *1* and *3*) and 7 (lane *2* and *4*) post-infection. Lanes *1* and *2* were treated with antiperforin antiserum and lanes *3* and *4* with preimmune serum. The nucleus-free lysates from 5×10^4 cell equivalents were analyzed on each lane. Autoradiography was performed for 24 h with intensifying screens.

fact present in $CD8^+$ lymphocytes that have been primed in vivo during the course of LCMV infection. The presence of massive numbers of $CD8^+$ cells in LCMV-infected tissues, as shown here, is consistent with the notion introduced in the past that $CD8^+$ cells are responsible for the immunopathology associated with this viral infection (11-14). In addition to $CD8^+$/perforin-positive cells, we also detected perforin in a small population of NK 1.1^+/asialo GM_1^+/$CD8^-$/$F4/80^-$ cells, presumably NK cells. In fact, NK cells have been shown to accumulate in tissues early on during LCMV infection, before $CD8^+$ cell infiltration (14, 25, 26). Thus, although a small number of the perforin-positive cells observed by us may represent NK cells, it is clear that the majority of the perforin-positive cells displays the CTL phenotype ($CD8^+$/NK 1.1^-/Thy-1^+).

It should be pointed out that perforin was detected primarily in $CD8^+$ lymphocytes displaying the LGL morphology. It is thus possible that in addition to being present in NK cells, perforin is primarily associated with LGL-like CTL undergoing blastogenesis, as suggested earlier (27). This finding is not surprising since all perforin-containing CTL clones studied to date morphologically resemble LGL. The question remains as to whether LGL- or blast-like CTL play a significant role in cytolytic reactions carried out in vivo. Recent studies by Welsh and his colleagues (14, 28) and our results presented here suggest that blast-like CTL are particularly prominent during some viral infections. As many as 20-30% of $CD8^+$ cells may become LGL like in tissues of LCMV-infected animals (14, 28). This condition may reflect the acute inflammatory and stimulatory microenvironment surrounding CTL in a viral focus that may drive these cells to become more active killers as well as to proliferate vigorously. It remains to be seen whether pathological conditions other than viral infections may also result in the accumulation of LGL-like CTL carrying perforin. We are currently investigating the presence of perforin in CTL actively engaged in tumor rejection in vivo.

With the cloning of mouse and human perforin (29-32), and several lymphocyte-specific serine esterases (33-40), it is now possible to carry out detailed in situ hybridization studies on diseased tissues in which CTL are thought to play a role in immunopathogenesis. Initial tissue hybridization studies, using serine esterase HF as probe, have already been performed by Weissman and his colleagues (41, 42). The combination of cDNA probe hybridization and antibody staining should provide a wealth of information regarding the distribution of CTL in various immunological disorders.

Summary

CTL and NK cells cultured in vitro have been shown to contain a cytolytic pore-forming protein (PFP/perforin/cytolysin). To date, it has not been determined whether perforin is expressed by CTL that have been primed in vivo. Here, we have infected mice with two strains of lymphocytic choriomeningitis virus (LCMV), one of which mainly produces choriomeningitis and, the other, hepatitis. Brain and liver cryostat sections obtained from LCMV-infected mice were stained for various lymphocyte markers, including perforin. We were able to detect a large accumulation of perforin antigen in $CD8^+$/Thy-1^+/asialo GM_1^+/$CD4^-$ lymphocytes, which in fact represent the main infiltrating cell type found in brain and liver sections obtained during the late acute stage of LCMV infection. Perforin was also detected in a smaller popu-

lation of CD8⁻/asialo GM_1^+/NK 1.1^+/F480⁻ cells, presumably corresponding to NK cells. Perforin-positive cells were found to have the morphology of blasts or large granular lymphocytes (LGL). These observations, together with in vitro studies performed in the past, indicate that perforin may be associated exclusively with LGL-like CTL blasts and NK cells. Our results demonstrate for the first time the presence of perforin in CTL that have been primed in vivo and suggest that perforin-positive CTL may be directly involved in producing the immunopathology associated with the LCMV infection.

References

1. Henkart, P. A. 1985. Mechanism of lymphocyte-mediated cytotoxicity. *Annu. Rev. Immunol.* 3:31.
2. Podack, E. R. 1985. The molecular mechanism of lymphocyte-mediated cytotoxicity. *Immunol. Today.* 6:21.
3. Young, J. D.-E, and Z. A. Cohn. 1987. Cellular and humoral mechanisms of cytotoxicity: structural and functional analogies. *Adv. Immunol.* 41:269.
4. Tschopp, J., and C. V. Jongeneel. 1988. Cytotoxic T lymphocyte mediated lysis. *Biochemistry.* 27:2641.
5. Dennert, G., C. G. Anderson, and G. Prochazka. 1987. High activity of N-alpha-benzyloxycarbonyl-L-lysine thiobenzyl ester serine esterase and cytolytic perforin in cloned cell lines is not demonstrable in in-vivo-induced cytotoxic effector cells. *Proc. Natl. Acad. Sci. USA.* 84:5004.
6. Berke, G., and D. Rosen. 1988. Highly lytic in vivo primed cytolytic T lymphocytes devoid of lytic granules and BLT-esterase activity acquire these constituents in the presence of T cell growth factors upon blast transformation in vitro. *J. Immunol.* 141:1429.
7. Clark, W. R. 1988. Perforin: a primary or auxiliary lytic mechanism? *Immunol. Today.* 9:101.
8. Berke, G. 1983. Cytotoxic T-lymphocytes. How do they function? *Immunol. Rev.* 72:5.
9. Ortaldo, J. R., and R. B. Herberman. 1984. Heterogeneity of natural killer cells. *Annu. Rev. Immunol.* 2:359.
10. Trinchieri, G., and B. Perussia. 1984. Human natural killer cells: biologic and pathologic aspects. *Lab. Invest.* 50:489.
11. Zinkernagel, R. M., and P. C. Doherty. 1979. MHC-restricted cytotoxic T cells: studies on the biological role of polymorphic major transplantation antigens determining T cell restrictions-specificity, function and responsiveness. *Adv. Immunol.* 27:51.
12. Buchmeier, M. J., R. M. Welsh, F. J. Dutko, and M. B. A. Oldstone. 1980. The virology and immunobiology of lymphocytic choriomeningitis virus infection. *Adv. Immunol.* 30:275.
13. Allan, J. E., J. E. Dixon, and P. C. Doherty. 1987. Nature of the inflammatory process in the central nervous system of mice infected with lymphocytic choriomeningitis virus. *Curr. Top. Microbiol. Immunol.* 134:131.
14. Welsh, R. M. 1987. Regulation and role of large granular lymphocytes in arenavirus infections. *Curr. Top. Microbiol. Immunol.* 134:185.
15. Young, J. D.-E, Z. A. Cohn, and E. R. Podack. 1986. The ninth component of complement and the pore-forming protein (perforin 1) from cytotoxic T cells: structural, immunological, and functional similarities. *Science (Wash. DC).* 233:184.

16. Persechini, P. M., and J. D.-E. Young. 1988. The primary structure of the lymphocyte pore-forming protein perforin: partial amino acid sequencing and determination of iso-electric point. *Biochem. Biophys. Res. Commun.* 156:740.

17. Crowley, M., K. Inaba, M. Witmer-Pack, and R. M. Steinman. 1989. The cell surface of mouse dendritic cells: FACS analyses of dendritic cells from different tissues including thymus. *Cell. Immunol.* 118:108.

18. Koo, G. C., and J. R. Peppard. 1984. Establishment of monoclonal anti-NK 1.1 antibody. *Hybridoma.* 3:301.

19. Dutko, F. J., and M. B. A. Oldstone. 1983. Genomic and biological variation among commonly used lymphocytic choriomeningitis virus strains. *J. Gen. Virol.* 64:1689.

20. Young, L. H. Y., and Dowling, J. E. 1984. Monoclonal antibodies distinguish subtypes of retinal horizontal cells. *Proc. Natl. Acad. Sci. USA.* 81:6255.

21. Oldstone, M. B. A., P. Blount, P. J. Southern, and P. W. Lampert. 1986. Cytoimmunotherapy for persistant virus infection reveals a unique clearance pattern from the central nervous system. *Nature (Lond.).* 321:239.

22. Allan, J. E., and P. C. Doherty. 1986. Natural killer cells contribute to inflammation but do not appear to be essential for the induction of clinical lymphocytic choriomeningitis. *Scand. J. Immunol.* 24:153.

23. Habu, S., H. Fukui, K. Shimura, M. Kasai, Y. Nagai, K. Okumura, and N. Tamaoki. 1981. In vivo effects of anti-asialo GM_1. Reduction of NK activity and enhancement of transplanted tumor growth in nude mice. *J. Immunol.* 127:34.

24. Yang, H., G. Yogeeswaran, J. F. Bukowski, and R. M. Welsh. 1985. Expression of asialo GM_1 and other antigens and glycolipids on natural killer cells and spleen leukocytes in virus-infected mice. *Nat. Immun. Cell Growth Regul.* 4:21.

25. Kiessling, R., and H. Wigzell. 1978. An analysis of the murine NK cell as to structure, function, and biological relevance. *Immunol. Rev.* 44:165.

26. Biron, C. A., and R. M. Welsh. 1982. Blastogenesis of natural killer cells during viral infection in vivo. *J. Immunol.* 129:2788.

27. Young, J. D.-E, and C.-C. Liu. 1988. Multiple mechanisms of lymphocyte-mediated killing. *Immunol. Today.* 9:140.

28. Biron, C. A., R. J. Natuk, and R. M. Welsh. 1986. Generation of large granular T lymphocytes in vivo during viral infection. *J. Immunol.* 136:2280.

29. Shinkai, Y., K. Takio, and K. Okumura. 1988. Homology of perforin to the ninth component of complement (C9). *Nature (Lond.).* 334:525.

30. Lichtenheld, M. G., K. J. Olsen, P. Lu, D. M. Lowrey, A. Hameed, H. Hengartner, and E. R. Podack. 1988. Structure and function of human perforin. *Nature (Lond.).* 335:448.

31. Lowrey, D. M., T. Aebischer, K. Olsen, M. Lichtenheld, F. Rupp, H. Hengartner, and E. R. Podack. 1989. Cloning, analysis, and expression of murine perforin 1 cDNA, a component of cytolytic T-cell granules with homology to complement component C9. *Proc. Natl. Acad. Sci. USA.* 86:247.

32. Kwon, B. S., M. Wakulchik, C.-C. Liu, P. M. Persechini, J. A. Trapani, A. K. Haq, Y. Kim, and J. D.-E Young. 1989. The structure of the mouse lymphocyte pore-forming protein perforin. *Biochem. Biophys. Res. Commun.* 158:1.

33. Gershenfeld, H. K., and I. L. Weissman. 1986. Cloning of a cDNA for a T cell-specific serine protease from a cytotoxic T lymphocyte. *Science (Wash. DC).* 232:854.

34. Lobe, C. G., B. B. Finlay, W. Paranchych, V. H. Paetkau, and R. C. Bleackley. 1986. Novel serine proteases encoded by two cytotoxic T lymphocyte-specific genes. *Science (Wash. DC).* 232:858.

35. Brunet, J.-F., M. Dosseto, F. Denizot, M.-G. Mattei, W. R. Clark, T. M. Haqqi, P. Ferrier, M. Nabholz, A.-M. Schmitt-Verhulst, M.-F. Luciani, and P. Golstein. 1986. The inducible cytotoxic T-lymphocyte-associated gene transcript CTLA-1 sequence and gene

localization to mouse chromosome 14. *Nature (Lond.)*. 322:268.

36. Kwon, B. S., G. S. Kim, M. B. Prystowsky, D. W. Lancki, D. E. Sabath, J. Pan, and S. M. Weissman. 1987. Isolation and initial characterization of multiple species of T-lymphocyte subset cDNA clones. *Proc. Natl. Acad. Sci. USA*. 84:2896.

37. Jenne, D., C. Rey, D. Masson, K. K. Stanley, J. Jerz, G. Plaetinek, and J. Tschopp. 1988. cDNA cloning of granzyme C, a granule-associated serine protease of cytolytic T lymphocytes. *J. Immunol.* 140:318.

38. Jenne, D., C. Rey, J. Haefliger, B. Qiao, P. Groscurth, and J. Tschopp. 1988. Identification and sequencing of cDNA clones encoding the granule-associated serine proteases granzyme D, E and F of cytolytic T lymphocytes. *Proc. Natl. Acad. Sci. USA*. 85:4814.

39. Trapani, J. A., J. L. Klein, P. C. White, and B. Dupont. 1988. Molecular cloning of an inducible serine esterase gene from human cytotoxic lymphocytes. *Proc. Natl. Acad. Sci. USA*. 85:6924.

40. Kwon, B. S., D. Kestler, E. Lee, M. Wakulchik, and J. D.-E Young. 1988. Isolation and sequence analysis of serine protease cDNAs from mouse cytolytic T lymphocytes. *J. Exp. Med.* 168:1839.

41. Mueller, C., H. K. Gershenfeld, G. G. Lobe, C. Y. Okada, R. C. Bleacklyey, and I. L. Weissman. 1988. A high proportion of T lymphocytes that infiltrate H-2-incompatible heart allografts in vivo express genes encoding cytotoxic cell-specific serine proteases, but do not express the MEL-14-defined lymph node homing receptor. *J. Exp. Med.* 167:1124.

42. Wood, G. W., C. Mueller, R. A. Warnke, and I. L. Weissman. 1988. In situ localization of HuHF serine protease mRNA and cytotoxic cell-associated antigens in human dermatoses. *Am. J. Pathol.* 133:218.